

International Journal of Exergy

ISSN online: 1742-8300 - ISSN print: 1742-8297
<https://www.inderscience.com/ijex>

Energy and exergy analysis of a steam power plant to replace the boiler with a heat recovery steam generator

Mahdi Mohseni, Hamid-Reza Bahrami, Mohammad Sadegh Leili

DOI: [10.1504/IJEX.2024.10061715](https://doi.org/10.1504/IJEX.2024.10061715)

Article History:

Received:	27 July 2023
Last revised:	17 November 2023
Accepted:	18 November 2023
Published online:	01 February 2024

Energy and exergy analysis of a steam power plant to replace the boiler with a heat recovery steam generator

Mahdi Mohseni*, Hamid-Reza Bahrami and
Mohammad Sadegh Leili

Department of Mechanical Engineering,
Qom University of Technology,
Qom 37181 46645, P.O. Box 37195-1519, Iran
Email: m.mohseni@qut.ac.ir
Email: taleshbahrami@qut.ac.ir
Email: sadeq.leili@gmail.com

*Corresponding author

Abstract: This research aims to optimise the power production of a thermal power plant in Iran by replacing the existing boiler with a heat recovery steam generator. A comprehensive study of the existing steam cycle and the proposed combined system reveals that the boiler, turbine, and condenser have the highest exergy destruction rates. The six heaters and boiler contribute 25% and 70% of the turbine input energy, respectively. The inlet temperatures of HP and IP turbines have the largest influence on the efficiency. The combined cycle analysis shows that first and second-law efficiencies can be increased by 27% and 26%, respectively.

Keywords: energy; exergy; thermal power plant; steam cycle; combined cycle; first law efficiency; second law efficiency; heat recovery; steam generator; turbine; boiler.

Reference to this paper should be made as follows: Mohseni, M., Bahrami, H-R. and Leili, M.S. (2024) 'Energy and exergy analysis of a steam power plant to replace the boiler with a heat recovery steam generator', *Int. J. Exergy*, Vol. 43, No. 1, pp.1–20.

Biographical notes: Mahdi Mohseni is an Assistant Professor at the Qom University of Technology since 2011. He completed his university studies in Mechanical Engineering, Fluid Mechanics, at the K.N. Toosi University of Technology in Tehran, Iran. Most of his research work is related to the CFD modelling of convection heat transfer in the turbulent flow of supercritical fluids using RANS models. Currently, his research work is focused on turbulent flow and turbulence modelling as well as new and renewable energies.

Hamid-Reza Bahrami is an Assistant Professor at Qom University of Technology. He received his PhD in Mechanical Engineering in 2018 from Iran University of Science and Technology. With a focus on heat transfer, nanofluids, porous media, PCM, thermodynamics, thermoeconomics, and battery thermal management, he brings expertise in these areas to his research and teaching activities. His work aims to advance the understanding and applications of these fields, contributing to the broader scientific community.

Mohammad Sadegh Leili received his Master's in Mechanical Engineering (Fluid Mechanics) from Qom University of Technology in 2021. He is currently working as an Engineer in the Montazer Ghaem thermal power plant.

1 Introduction

In recent years, energy and exergy analysis have been implemented as practical techniques in the optimisation of thermodynamic systems (Davoodi et al., 2023; Atiz et al., 2023; Mohseni and Bazargan, 2014). This procedure, which is based on the first and second laws of thermodynamics, can be used to identify the rates of irreversibility of different components of a system (Mert et al., 2023; Khaliq et al., 2019). Thermal power plants based on fossil fuels are one of the main culprits of the pollutant emission systems as well as the primary consumers of underground resources (Vakilabadi et al., 2018; Khaleel et al., 2022; Deymi-Dashtebayaz et al., 2019). However, it is predicted that fossil fuels will continue to be the primary energy source for power plants until at least 2040 due to their affordable price and abundant availability (Khaleel et al., 2022). Therefore, every effort should be made to improve current fossil fuel power plants before introducing new cost-effective systems based on renewable energy resources (Pinto et al., 2022).

Previous research shows that boiler and condenser have the highest exergy and energy losses in steam power plants (Azubuike et al., 2023; Siddiqui, 2021). For example, in a study by Aljundi, 2009, the boiler accounts for 77% of the total exergy losses. Therefore, the focus should be on improving this equipment by reducing exergy losses through solutions such as using heat recovery steam generators (HRSGs) and combined cycle power plants (Manesh et al., 2020; Surywanshi et al., 2020), preheating combustion air entering the boiler (Aljundi, 2009), improving steam turbine efficiency by increasing feedwater pressure, changing the arrangement of water heaters (Naserabad et al., 2019), recovering heat, exergy, and water in the blowdown process (Vakilabadi et al., 2018), using solar panels in addition to/instead of water heaters (Adibhatla and Kaushik, 2017).

This study aims to enhance the performance of a thermal power plant in Iran through energy and exergy analysis. The plant consists of gas and steam units operating separately. The study examines the effects of parameters on the steam power plant's efficiency, such as boiler outlet pressure, turbine inlet temperature, and condenser vacuum pressure. The main objective is to explore the possibility of replacing the steam boiler with a HRSG using gas turbine waste heat.

2 Introducing the power plant (steam cycle)

The system under study is the Montazer Ghaem, a thermal power plant located in the Shahriar region of Alborz Province in Iran. This power plant has four steam units each with a nominal capacity of 156 MW, and six gas units each with a nominal capacity of 116 MW. The first steam unit of the plant was commissioned and connected to the network in 1971. The other three units were completed and connected to the network in 1973. Two gas units were also connected to the grid in 1992, and the third to sixth gas

units in 1993. The fuel consumed by the power plant is natural gas with specifications given in Table 1. In this table, \dot{v}_f is the volume flow of fuel in the nominal conditions.

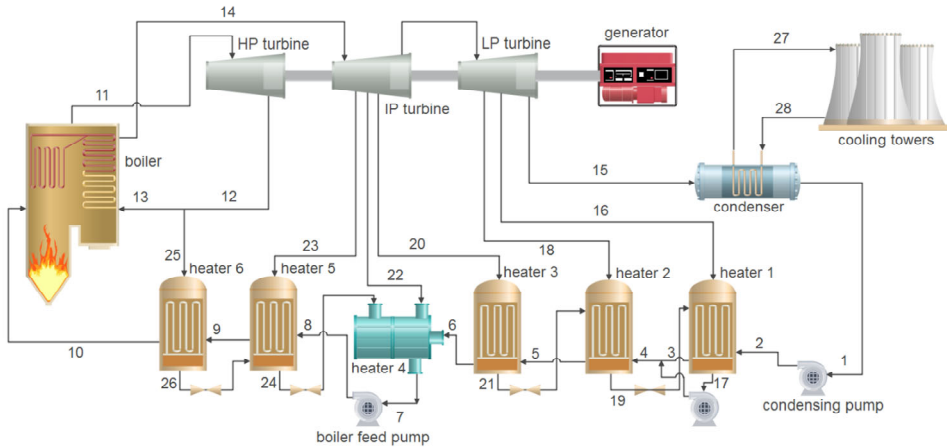
Table 1 Specifications and chemical composition of power plant fuel consumption

<i>Gas properties</i>	<i>Value</i>
CH ₄	80.2%
C ₂ H ₆	6.7%
CO ₂	0.8%
N ₂	12.3%
HHV ¹	34,725.44 kJ/m ³
\dot{v}_f	46.666 m ³ /hour

Note: ¹Higher heating value.

The boiler of each unit is of drum type with a reheating system, pressurised furnace, and gas-circulating fan. The steam power plant consists of three high, intermediate, and low-pressure (HP, IP, and LP) turbines whose axis is coupled with an electric generator. The power plant's condenser is of the water-cooled type and has an absolute pressure of 8.46 kPa. Heat is removed from the condenser by a wet cooling tower. A schematic diagram of the power plant steam cycle is shown in Figure 1.

Figure 1 Flow diagram of the steam cycle (see online version for colours)



The steam cycle works as follows. The steam leaving the low-pressure turbine enters the condenser at point 15 and leaves it after complete condensation. The liquid water then enters the condensing pump at point 1, which provides the necessary pressure for the water to flow to heater number 4. The condensed water then enters heater number 1 (point 2), which is heated by the steam from the low-pressure turbine (line 16). In the next step, the liquid water, after mixing with the condensed water received from the first and second heaters, enters heater number 2 (point 4). The hot steam that enters the jacket of this heater is also supplied by the low-pressure turbine (line 18). The heated water then enters heater number 3 (point 5). The steam for heater 3 is taken from the medium-pressure turbine (line 20). After passing the closed heaters 1, 2 and 3, the condensed

water enters the open heater 4 (point 6). This heater makes the chemical conditions of the water favourable and prevents dissolved gases from entering the turbine. In addition, this heater is located at a high level to provide the required head to the boiler feed pump to prevent the cavitation phenomenon in the pump. The output from heater 4 flows to the boiler feed pump (point 7). The pump provides the necessary head to deliver water to the boiler drum. The extracted steam for heater 5 is taken from the middle stage of the medium-pressure turbine (line 23), and the required hot steam for heater 6 is taken from the reverse reheat path (line 25). The temperature of the water at the outlet of heater 6 exceeds 232°C at a pressure of 206.84 bar (point 10). Then the condensed water enters the boiler and turns into superheated steam with a temperature of about 538°C. The steam then enters the high-pressure turbine. The output steam from the high-pressure turbine (point 12) is returned to the boiler for reheating (point 13). After reheating, the steam enters the medium-pressure turbine from the cold-reheat path to the hot-reheat path (point 14). After passing through the medium-pressure turbine, the steam enters the low-pressure turbine. By condensing the steam in the condenser, the water enters the cycle again and repeats its path.

3 Governing equations

This section gives the governing equations required to perform the power plant's energy and exergy analysis. These equations include the conservation of mass, energy, and exergy balances and the first and second law efficiencies for an open system in steady-state conditions (Cengel et al., 2019):

Continuity equation:

$$\sum \dot{m}_i = \sum \dot{m}_o \quad (1)$$

The first law of thermodynamics:

$$\dot{Q} + \sum \dot{m}_i \left(h_i + \frac{V_i^2}{2} + gz_i \right) = \dot{W} + \sum \dot{m}_o \left(h_o + \frac{V_o^2}{2} + gz_o \right) \quad (2)$$

The first law efficiency of every component or overall system is obtained as the ratio of the output energy to the input energy as equation (3).

$$\eta_1 = \frac{\text{Energy}_{\text{output}}}{\text{Energy}_{\text{input}}} \quad (3)$$

The exergy analysis of a system is expressed by the second law of thermodynamics. The exergy balance for a heating system in steady flow is stated as follows.

$$\sum \left(1 - \frac{T_0}{T} \right) \dot{Q} + \sum \dot{m}_i \psi_i = \dot{W} + \sum \dot{m}_o \psi_o + T_0 \dot{S}_{\text{gen}} \quad (4)$$

where

$$EX = \dot{m} \psi = \dot{m} \left[(h - h_o) - T_o (s - s_o) + \frac{V^2}{2} + gz \right]$$

The second law efficiency is stated as

$$\eta_2 = \frac{\text{Exergy}_{\text{recovered}}}{\text{Exergy}_{\text{expended}}} = 1 - \frac{\text{Exergy}_{\text{destroyed}}}{\text{Exergy}_{\text{expended}}} \quad (5)$$

In the above equations, EX is exergy rate (W), h is specific enthalpy (kJ/kg), \dot{m} is the mass flow rate (kg/s), \dot{Q} is rate of heat transfer (W), s is specific entropy (J/kg.K), \dot{S}_{gen} is the entropy generation (J/kg.°C), T is the temperature (°C), V is the velocity (m/s), \dot{W} is the power (W), z is the elevation (m), η is efficiency, and ψ is the specific exergy (kJ/kg). Also, the subscript 0 refers to ambient conditions.

The above-mentioned equations are in their complete form, which can be simplified for each component of the power plant. The energy and exergy equations for each power plant component are presented in Table 2. The following assumptions are used in deriving these equations.

- 1 All components except the condenser are assumed to be adiabatic.
- 2 Changes in the kinetic and potential energies of the fluid are negligible.
- 3 The leakage of the working fluid in different components is neglected.
- 4 Heaters are assumed to work in ideal conditions.

In Table 2, $\dot{e}_i = \dot{m}_i h_i$ is the rate of energy transfer that is flowing with mass and \dot{X} is the exergy destruction rate (kJ/hr). Also, the \dot{Q}_b in the boiler equation is the energy required to bring the steam to the required temperature at the turbine inlet. However, the total energy entering the boiler is much greater. The energy efficiency of the steam boiler is calculated as follows (Khaleel et al., 2022).

$$\eta_{\text{boiler}} = \frac{\dot{Q}_b}{\dot{Q}_{b,\text{in}}} \quad (6)$$

where $\dot{Q}_{b,\text{in}} = \dot{v}_f \rho_f \text{HHV}$ is the total input energy entering the boiler, HHV is the higher heating value of the fuel and \dot{v}_f is its volume flow rate which can be obtained from Table 1. The difference between the two values of \dot{Q}_b and $\dot{Q}_{b,\text{in}}$ is wasted to the environment mainly through the boiler chimney.

Two types of pumps are used in the studied cycle, including condensing pump and boiler feed water pump, BFP, which are of centrifugal type. There are also two types of heaters: closed-feed water and open-feed water heaters. In the closed-feed water heater (heaters No. 1, 2, 3, 5, and 6), cold and hot flows do not mix, while in the open-feed heater, i.e., heater No. 4, cold and hot flows are mixed. In addition, the steam turbine consists of three high-, medium-, and low-pressure sections, as previously mentioned. The energy and exergy equations for the turbine have been written for all three sections as a whole, taking into account the vapours extracted from the turbine for the heaters.

The total energy and exergy efficiencies of the power plant are expressed as follows.

$$\eta_{1,\text{steam cycle}} = \frac{\dot{W}_{\text{turbine}} - \dot{W}_{\text{pumps}}}{\dot{e}_f} \quad (7)$$

$$\eta_{2, \text{steam cycle}} = \frac{\dot{W}_{\text{turbine}}}{\sum \dot{X}} \quad (8)$$

where $\sum \dot{X}$ is the sum of the total exergy destruction rate.

Table 2 The energy and exergy balance equations and second law efficiencies for each component

<i>Equipment</i>	<i>Energy balance</i>	<i>Exergy balance</i>	<i>Second law efficiency, η_2</i>
Condensing pump	$\dot{W}_{\text{cond.p}} = \dot{e}_2 - \dot{e}_1$	$EX_1 + \dot{W}_{\text{cond.p}} = EX_2$ $+ \dot{X}_{\text{cond.p}}$	
Boiler feed water pump	$\dot{W}_{\text{BFP}} = \dot{e}_8 - \dot{e}_7$	$EX_7 + \dot{W}_{\text{BFP}}$ $= EX_8 + X_{\text{BFP}}$	
Heater 1	$\dot{e}_2 + \dot{e}_{16} + \dot{e}_{19}$ $= \dot{e}_3 + \dot{e}_{17}$	$EX_2 + EX_{16} + EX_{19} =$ $EX_3 + EX_{17} + \dot{X}_{\text{heater1}}$	$\eta_{2,\text{heater1}} = \frac{EX_3 - EX_2}{EX_{16} + EX_{19} - EX_{17}}$
Heater 2	$\dot{e}_4 + \dot{e}_{18} + \dot{e}_{21}$ $= \dot{e}_5 + \dot{e}_{19}$	$EX_4 + EX_{18} + EX_{21} =$ $EX_5 + EX_{19} + \dot{X}_{\text{heater2}}$	$\eta_{2,\text{heater2}} = \frac{EX_5 - EX_4}{EX_{18} + EX_{21} - EX_{19}}$
Heater 3	$\dot{e}_5 + \dot{e}_{20} = \dot{e}_6 + \dot{e}_{21}$	$EX_5 + EX_{20} = EX_6$ $+ EX_{21} + \dot{X}_{\text{heater3}}$	$\eta_{2,\text{heater3}} = \frac{EX_6 - EX_5}{EX_{20} - EX_{21}}$
Heater 4	$\dot{e}_6 + \dot{e}_{22} + \dot{e}_{24} = \dot{e}_7$	$EX_6 + EX_{22} + EX_{24} =$ $EX_7 + \dot{X}_{\text{heater4}}$	$\eta_{2,\text{heater4}} = \frac{EX_7 - EX_6}{EX_{22} + EX_{24}}$
Heater 5	$\dot{e}_8 + \dot{e}_{23} + \dot{e}_{26}$ $= \dot{e}_9 + \dot{e}_{24}$	$EX_8 + EX_{23} + EX_{26} =$ $EX_9 + EX_{24} + \dot{X}_{\text{heater5}}$	$\eta_{2,\text{heater5}} = \frac{EX_9 - EX_8}{EX_{23} + EX_{26} - EX_{24}}$
Heater 6	$\dot{e}_9 + \dot{e}_{25} = \dot{e}_{10} + \dot{e}_{26}$	$EX_9 + EX_{25} = EX_{10}$ $+ EX_{26} + \dot{X}_{\text{heater6}}$	$\eta_{2,\text{heater6}} = \frac{EX_{10} - EX_9}{EX_{25} - EX_{26}}$
Boiler	$\dot{e}_{10} + \dot{e}_{13} + \dot{Q}_b$ $= \dot{e}_{11} + \dot{e}_{14}$	$EX_{10} + EX_{13} = EX_{11}$ $+ EX_{24} + \dot{X}_{\text{boiler}}$	$\eta_{2,\text{boiler}} = \frac{EX_{11} + EX_{14} - EX_{10} - EX_{13}}{\dot{v}_f \rho_f \psi_f}$ and $\psi_f = 49,825.44 \text{ kJ/kg}$
Steam turbine	$\dot{e}_{11} + \dot{e}_{14} = \dot{e}_{12} + \dot{e}_{15}$ $+ \dot{e}_{16} + \dot{e}_{18} + \dot{e}_{20}$ $+ \dot{e}_{22} + \dot{e}_{23} + \dot{W}_{\text{turbine}}$	$EX_{11} + EX_{14} = EX_{12}$ $+ EX_{15} + EX_{16} + EX_{18}$ $EX_{20} + EX_{22} + EX_{23}$ $+ \dot{X}_{\text{turbine}}$	$\eta_{2,\text{turbine}} = \frac{\dot{W}_{\text{turbine}}}{EX_{\text{tur}}}$ where $EX_{\text{turb}} = EX_{11} + EX_{14} - EX_{12}$ $- EX_{15} - EX_{16} - EX_{18} - EX_{20}$
Condenser	$\dot{Q}_{\text{loss.cond}} = \dot{e}_{15}$ $- \dot{e}_1 = \dot{e}_{28} - \dot{e}_{27}$	$EX_{15} + EX_{27} = EX_1$ $+ EX_{128} = \dot{X}_{\text{cond}}$	$\eta_{2,\text{cond}} = \frac{EX_{28} - EX_{27}}{EX_{15} - EX_1}$
Expansion valve	$h_0 = h_i$	$EX_i = EX_o + \dot{X}_{\text{cond}}$	

4 Results and discussion

This section presents the results of solving the equations governing the various components of the power plant. The equations have been written in the EES, the Engineering Equation Solver (Klein and Alvarado 2018). After analysing the nominal conditions of the steam cycle in the first part, the following parts evaluate the effects of various factors that affect the performance of the cycle, such as the use of a gas turbine unit to establish a combined cycle, the effect of the boiler outlet temperature and pressure, and the vacuum pressure of the condenser.

Table 3 Thermodynamic properties of different points of the cycle

Point	p	T	h	s	ψ	\dot{m}	\dot{e}	EX
	bar	$^{\circ}C$	kJ/kg	$kJ/(kg \cdot ^{\circ}C)$	kJ/kg	kg/hr	MJ/hr	MJ/hr
1	0.093	42.56	178.196	0.1871145	1.988738	3.775E+05	67,281.2	750.8
2	8.191	42.61	179.219	0.187373	2.816797	3.775E+05	67,661.0	1,063.5
3	8.191	92.78	389.141	0.3778473	28.79599	3.775E+05	146,969.9	10,877.7
4	8.191	92.78	389.141	0.3778473	28.79599	4.019E+05	156,465.4	11,574.0
5	8.191	130.8	550.101	0.5068115	64.96544	4.019E+05	221,035.1	26,112.7
6	8.191	149.7	630.814	0.5671586	87.4812	4.019E+05	253,530.9	35,165.1
7	8.191	171.4	725.25	0.6343544	116.9517	4.690E+05	339,940.3	54,831.5
8	210.4	174.6	750.138	0.6360343	140.2351	4.690E+05	351,651.5	65,740.8
9	203.4	198.9	855.739	0.7074944	176.8465	4.690E+05	401,133.8	82,906.6
10	199.9	236.3	1,022.98	0.8129402	242.3702	4.690E+05	479,630.3	113,630.0
11	125.1	537.8	3,444.82	2.0339658	1,483.529	4.690E+05	1,615,296.9	69,5601.1
12	31.34	346.7	3,105.22	2.0701481	1,109.739	4.690E+05	1,455,982.8	520,250.1
13	31.34	346.7	3,105.22	2.0701481	1,109.739	4.312E+05	1,338,871.1	478,469.7
14	28.2	537.8	3,544.84	2.2756123	1,350.248	4.708E+05	1,669,104.9	635,884.7
15	0.093	44.5	2,472.55	2.4151728	142.7704	3.775E+05	933,095.1	53,903.0
16	0.778	133	2,744.69	2.3621915	467.7604	2.437E+04	66,880.3	11,394.6
17	0.778	92.78	388.676	0.3779765	28.07493	2.437E+04	9,469.2	684.0
18	2.765	239.3	2,947.05	2.319548	711.061	2.651E+04	78,127.2	18,853.9
19	2.765	130.8	549.636	0.5069408	64.43045	3.977E+04	21,860.8	2,562.7
20	4.716	308.1	3,081.96	2.319548	844.5739	1.326E+04	40,862.5	11,204.7
21	4.716	149.7	630.581	0.5672878	87.15556	1.326E+04	8,363.5	1,156.3
22	8.191	384.2	3,233.15	2.3182558	998.7883	1.252E+04	40,503.8	12,513.0
23	14.99	466.9	3,400.63	2.307918	1,176.961	1.678E+04	57,068.2	19,740.2
24	14.99	198.2	844.341	0.714214	159.0525	5.441E+04	45,947.9	8,653.6
25	31.34	346.7	3,105.22	2.0701481	1,109.739	3.763E+04	116,900.6	41,759.3
26	31.34	236.3	1,019.72	0.8234072	228.9723	3.763E+04	38,383.1	8,617.7
27	2.068	28.33	118.952	0.1276721	0.184801	1.953E+07	2,323,242.1	3,609.4
28	2.068	38.94	163.286	0.1722539	1.429333	1.953E+07	3,189,446.4	27,916.9

4.1 Steam cycle (nominal conditions)

In this part, the steam cycle is examined in nominal conditions. Table 3 shows the thermodynamic properties of different points of the cycle shown in Figure 1. These properties include pressure, temperature, enthalpy, entropy, mass flow rate, exergy, and rate of exergy.

As can be seen from Table 3, the highest pressures are related to points 8, 9, and 10, i.e., just after the main pump. The highest temperatures are associated with points 11 and 14 at the boiler outlet, i.e., the entrance to the high and medium-pressure turbines. The highest enthalpy occurs at point 14, where the steam enters the IP turbine. In addition, the highest entropy occurs at the outlet of the LP turbine and the inlet of the condenser, i.e., point 15. The highest exergy rate of the system belongs to point 11, the boiler outlet. The contribution of 6 heaters to the total energy required for the flow entering the turbine is 24.5%, and the contribution of the boiler is 70%. The most significant steam pressure drops occur in the HP turbine and the boiler, which are 93.77 bar and 74.46 bar, respectively. The maximum energy loss occurs in the condenser, which is 2,294.37 kJ/kg. For a better comparison, Figure 2 shows the enthalpy value at different points in the steam cycle. It is possible to see the contribution made by each heater and by the boiler to the heating of the water.

Figure 2 Enthalpy values at different points of the steam cycle (see online version for colours)

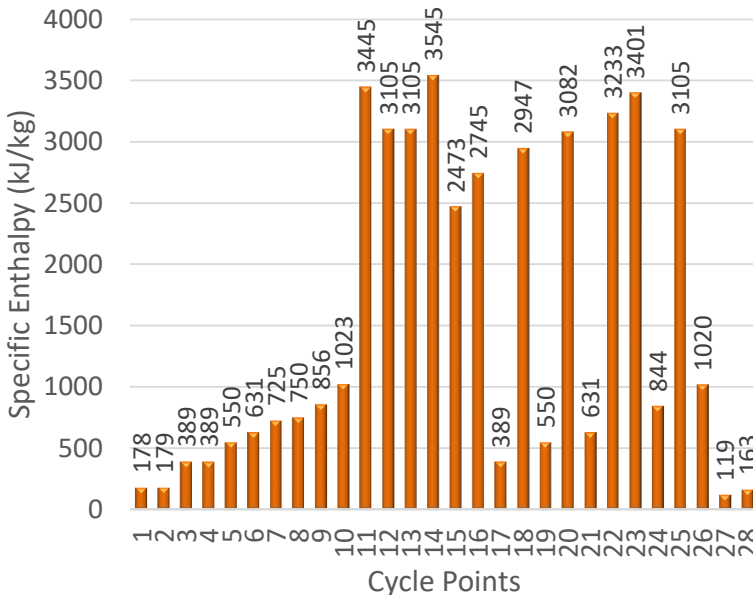
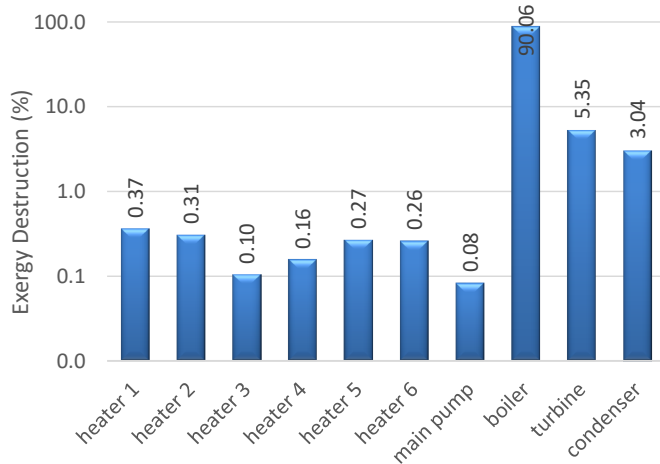


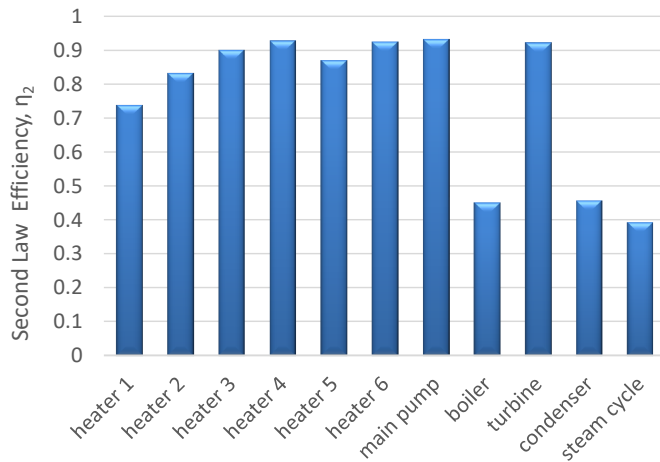
Figure 3(a) shows the contribution of the main components of the steam cycle to the exergy destruction rate. The results show that the highest exergy destruction rate occurs in the boiler with a value of 854.6 kJ/hr, which accounts for approximately 90% of the total exergy destruction rate of the steam cycle. This is in agreement with previous research (Erzen et al., 2022). The steam turbine ranks second and accounts for 50.8 kJ/hr, which is 5.35% of the total exergy destruction of the cycle. It is noteworthy that, unlike

the largest energy loss in the condenser, the exergy destruction rate of this equipment is 28.84 kJ/hr, only 3% of the total exergy destruction of the cycle.

Figure 3 Exergy analysis of different components of the steam cycle, (a) contribution of exergy destruction rate (b) second law efficiency



(a)



(b)

Figure 3(b) shows the second-law efficiency of different power plant components. It can be seen that the boiler and the condenser have the lowest efficiencies about 45%. Due to the high-temperature difference between the water and the combustion products, a large amount of exergy is lost in the boiler. Also, heaters 4 and 6, as well as the main pump and turbine, have the highest second-law efficiency, about 92%.

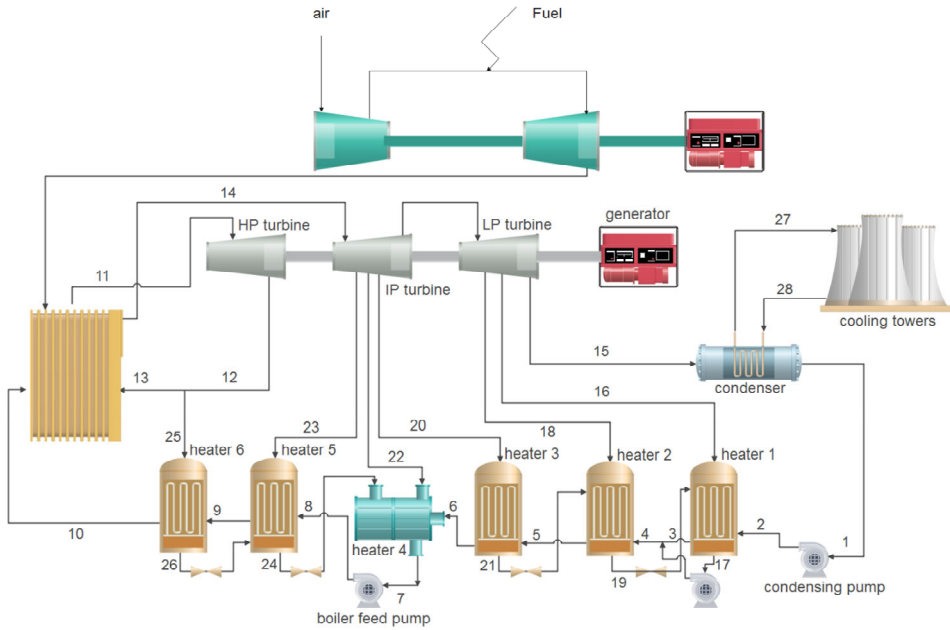
4.2 Combined cycle

To increase the overall efficiency of the steam power plant, a HRSG can be used instead of the boiler. For this purpose, hot exhaust gases from the gas turbine unit are used as input. The technical specifications of the gas turbine unit are given in Table 4. The schematic diagram of the resulting combined cycle is shown in Figure 4.

Table 4 Technical specifications of the gas turbine unit, model: Siemens SGT6-8000H

Quantity	Value	Unit
Output power	274	MW
Efficiency	40.16	---
Mass flow rate of combustion products	600	kg/s
Temperature of combustion products	893.150	K
Compressor pressure ratio	20	---

Figure 4 Steam and gas combined cycle flow diagram (see online version for colours)



The first and second law efficiencies of the combined cycle are given in equations (9) and (10).

$$\eta_{1,combined\ cycle} = \frac{\dot{W}_{st.turbine} + \dot{W}_{gas\ turbine}}{\dot{Q}_{Fuel, gas.turbine}} \tag{9}$$

$$\eta_{2,combined\ cycle} = \frac{\dot{W}_{st.turbine} + \dot{W}_{gas\ turbine}}{EX_{Fuel\ gas\ turbine}} \tag{10}$$

where $\dot{Q}_{Fuel, gas, turbine}$ is the energy released from the fuel consumed in the gas turbine. Also, $EX_{Fuel, gas, turbine} = \dot{m}_{fuel, gas, turbine} \times \psi_{fuel, gas, turbine}$ is the exergy of the fuel entering the combustion chamber of the gas turbine.

The results show that the first law efficiency increases from 34.74% in the steam cycle to 65.06% in the combined cycle. Similarly, the second law efficiency increases from 39.3% to 63.27%. It is worth noting that this improvement could also reduce the negative impact of the current steam cycle on global warming by reducing fossil fuel consumption and gas emissions.

The following sections show the effect of various parameters on the performance of both steam and combined cycles.

4.3 Effects of condenser vacuum pressure on power plant performance

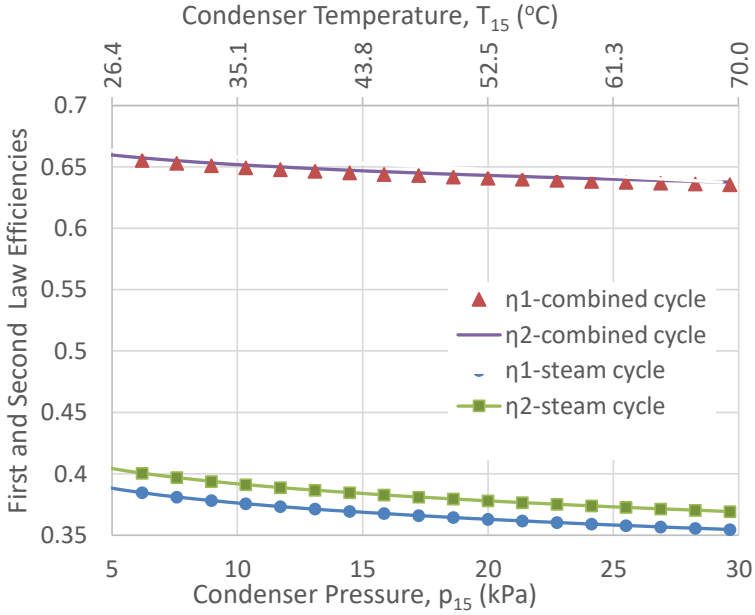
The humidity and temperature of the ambient air have a significant effect on wet cooling towers and consequently on the condenser vacuum pressure (Kapooria et al., 2008). In other words, increasing the humidity and temperature of the ambient air reduces the condenser vacuum pressure. It disturbs the steam condensation process and increases the condenser temperature. As a result, the useful work of the turbine is reduced. Figure 5(a) shows the first and second law efficiencies of both steam and combined cycles as a function of condenser vacuum pressure. In this figure, the lower horizontal axis shows the vacuum pressure and the upper axis shows the corresponding temperature. It can be seen that an increase in condenser pressure, which is equivalent to a decrease in condenser vacuum, reduces system efficiency. This means that increasing condenser pressure by about 27.58 kPa reduces system efficiency by about 5%. The same trend can be found in the literature (Arpit et al., 2021).

Detailed examination of the results shows that the condenser pressure change mainly affects three components, including the condenser, turbine, and heater 1, as shown in Figure 5(b). Although the vacuum pressure increase causes the exergy destruction rate of the turbine and heater 1 to decrease, it increases the exergy destruction rate of the condenser. It can be concluded that the exergy destruction of the condenser is predominant and increases the exergy destruction rate of the whole cycle.

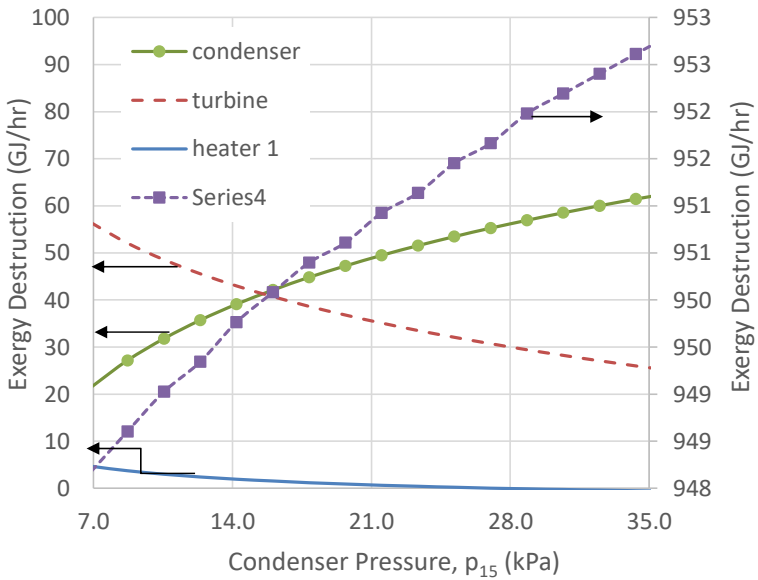
4.4 Effect of steam temperature entering the HP turbine

One of the most critical parameters affecting the overall performance of the cycle is the temperature or enthalpy of the steam entering the turbine. Figure 6 shows the effect of this parameter on the performance of the system. The nominal boiler outlet temperature is 537°C. It can be seen that both the first and second law efficiencies of both steam and combined cycles increase almost linearly with an increase in the inlet temperature of the HP turbine. A similar result was found in the literature (Rout et al., 2013). It can be seen that for each 275°C increase in this temperature, the first and second law efficiencies of the system increase by about 12% and 8%, respectively. Although structural and metallurgical restrictions limit the increase in this temperature, these issues may be resolved in the future.

Figure 5 Effect of condenser pressure for both steam and combined cycles, (a) the first and second law efficiencies (b) the exergy destruction rate of equipment and the steam cycle (see online version for colours)

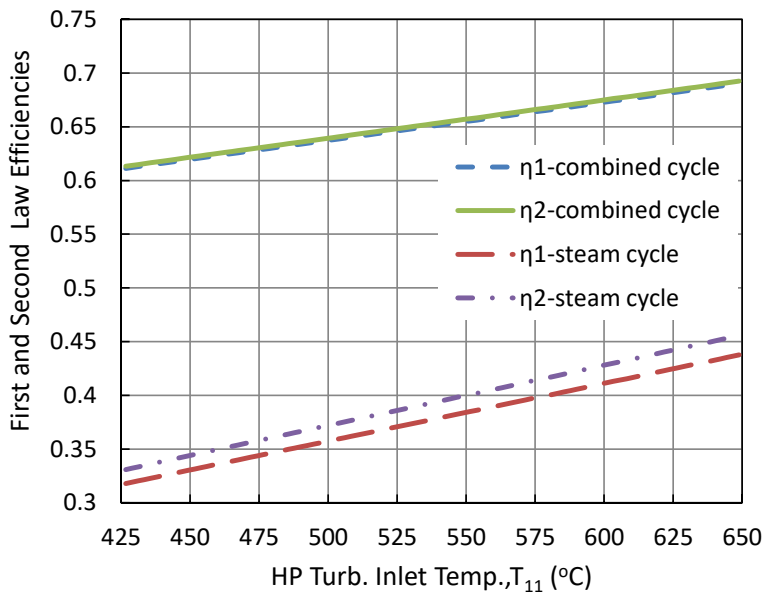


(a)



(b)

Figure 6 Effect of HP turbine inlet temperature on the first and second law efficiencies (see online version for colours)



The effects of the HP turbine inlet temperature on the exergy destruction rates of the main components of the cycle are shown in Figure 7. It can be observed that although the exergy destruction rate of the heaters, turbine and condenser increases with the increase of the mentioned temperature, it decreases in the boiler as the main exergy destructor equipment. Therefore, the total exergy destruction rate of the cycle also decreases as T_{11} increases.

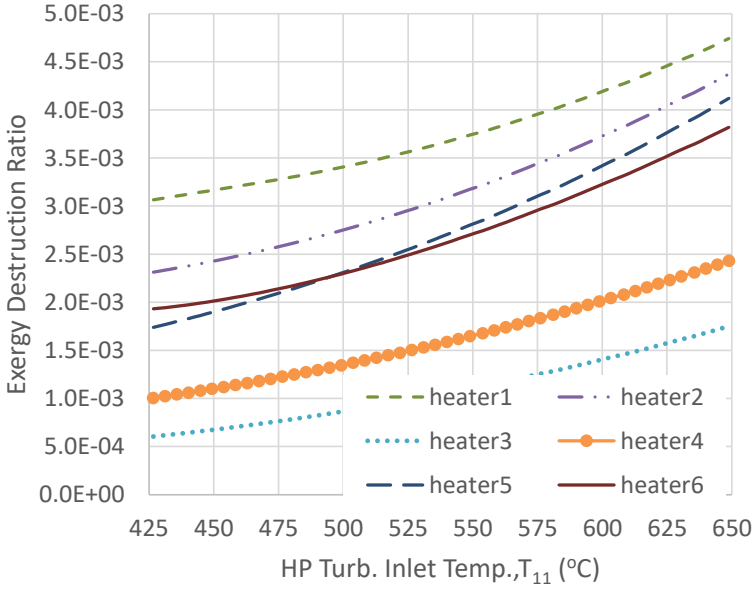
4.5 Effect of IP turbine inlet temperature

Another important parameter affecting cycle performance is the inlet temperature of the IP turbine. As shown in Figure 8(a), this factor has a significant effect on the first and second-law efficiencies. In other words, an increase of 200°C in the IP turbine inlet temperature improves the energy efficiency of the steam cycle by about 6%. This increase also mainly affects the boiler performance, which reduces the total exergy destruction rate, as shown in Figure 8(b).

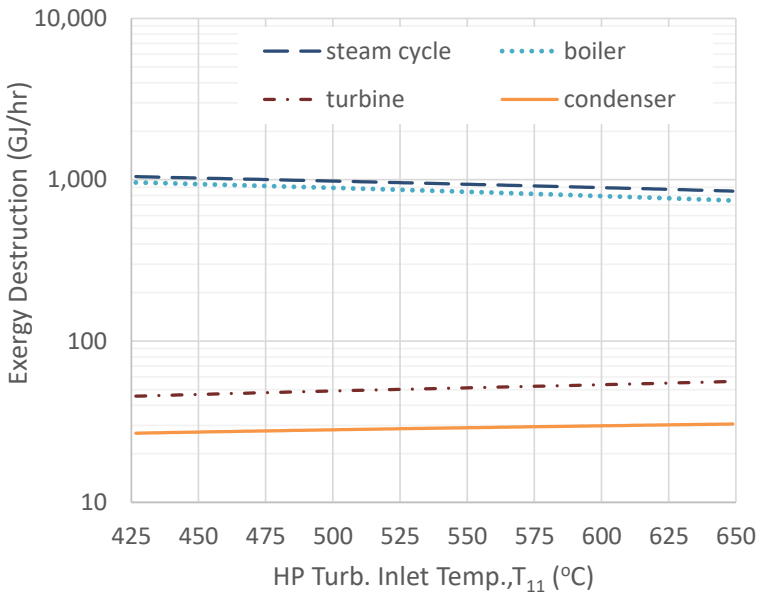
4.6 Effect of boiler outlet pressure

The effects of boiler outlet pressure on energy and exergy efficiencies are shown in Figure 9(a) for both steam and combined cycles. It can be seen that an increase in boiler outlet pressure of up to 100 bar increases the first and second law efficiencies by about 5% and 4%, respectively. The effect of varying the boiler outlet pressure on the total exergy destruction rate as well as on different equipment is shown in Figure 9(b). It is observed that the destruction rate increases for some equipment and decreases for others, including the boiler. In general, as the boiler outlet pressure increases, the total exergy destruction rate decreases.

Figure 7 Effect of HP turbine inlet temperature on exergy destruction rate, (a) heaters (b) main components and the cycle (see online version for colours)

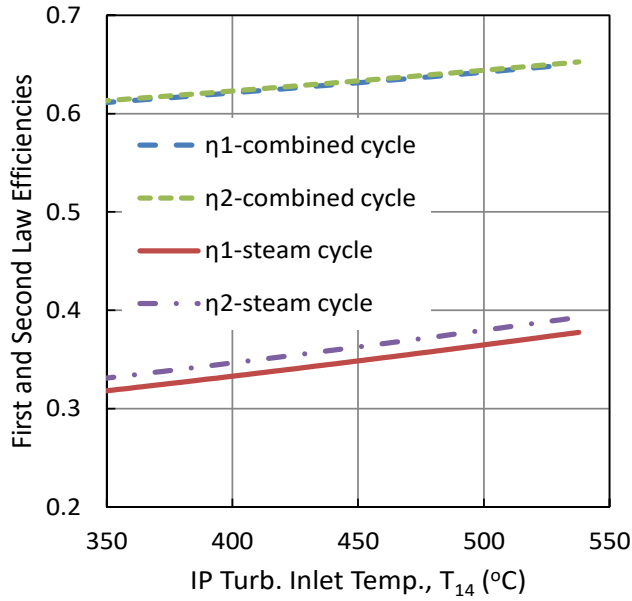


(a)

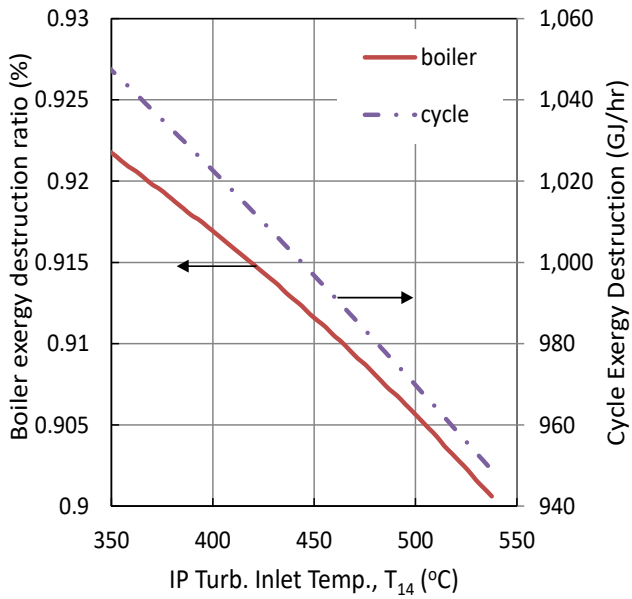


(b)

Figure 8 Effect of IP turbine inlet temperature, (a) first and second law efficiencies (b) total and boiler exergy destruction rate (see online version for colours)

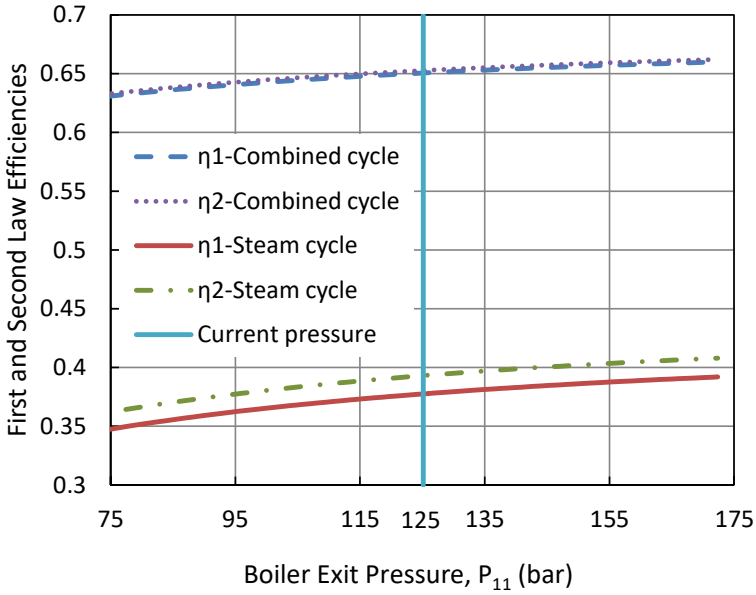


(a)

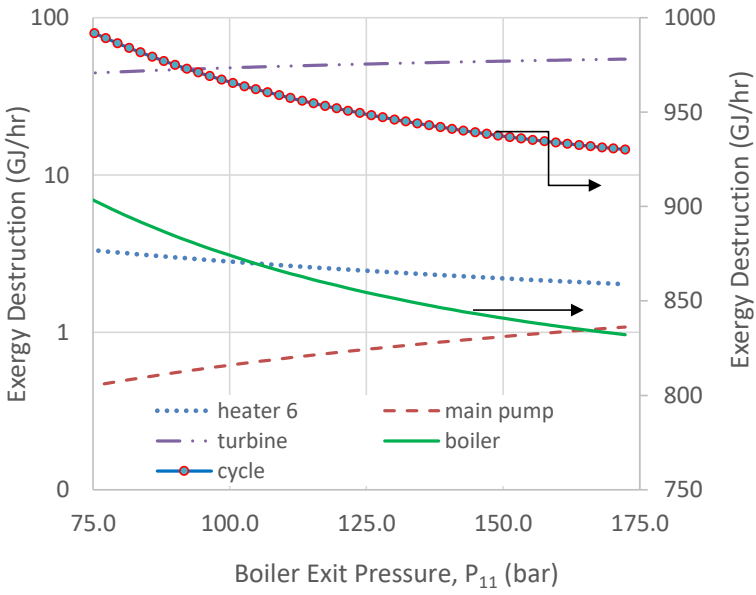


(b)

Figure 9 Effect of boiler output pressure, (a) first and second law efficiencies (b) exergy destruction rate of different components (see online version for colours)



(a)



(b)

4.7 Comparison of the effects of different parameters

It is necessary to know which of the aforementioned parameters has the greatest influence on the cycle performance. For this reason, Table 5 compares the first and second law efficiency results for a $\pm 20\%$ change in parameters. When one parameter is changed, other parameters remain fixed at their nominal conditions. It can be seen that the best performance is obtained when the T14, i.e., the inlet temperature of the IP turbine, is increased by 20%. These improvements are about 16% and 6% for steam and combined cycle efficiencies, respectively. It should be noted that the increase in T14, which is the reheat of the steam leaving the HP turbine, is accompanied by an increase in T11, i.e., $T14 = T11 = 649^\circ\text{C}$. Similarly, a 20% increase in T11, the inlet temperature to the HP turbine, improves the energy efficiency by about 5.4% and the second law efficiency by about 2.4%. These values for boiler outlet pressure are 2.3% and 0.9%, respectively.

Table 5 Effect of $\pm 20\%$ changes of some parameters on both steam and combined cycle efficiencies (see online version for colours)

Range	Value	Steam cycle				Combined cycle			
	T11 (°C)	η_1	Change (%)	η_2	%	η_1	%	η_2	%
-20%	427	0.318	-15.79	0.331	-15.80	0.611	-6.056	0.613	-6.05
Nominal	538	0.377		0.393		0.651		0.653	
+20%	649	0.398	5.41	0.414	5.39	0.664	2.060	0.666	2.05
	P11 (bar)								
-20%	100	0.365	-3.18	0.381	-3.18	0.643	-1.230	0.643	-1.55
Nominal	125	0.377		0.393		0.651		0.653	
+20%	150	0.386	2.31	0.402	2.29	0.656	0.876	0.658	0.87
	T14 (°C)								
-20%	427	0.341	-9.64	0.355	-9.64	0.627	-3.689	0.629	-3.69
Nominal	538	0.377		0.393		0.651		0.653	
+20%	649	0.438	15.95	0.456	15.95	0.690	6.102	0.693	6.10
	P15 (bar)								
-20%	0.075	0.381	1.06	0.397	1.04	0.653	0.400	0.655	0.40
Nominal	0.093	0.377		0.393		0.651		0.653	
+20%	0.112	0.377	-0.08	0.390	-0.87	0.648	-0.338	0.651	-0.34

It is useful to obtain the efficiency of the cycles when all the parameters are in the range of $\pm 20\%$ in the best conditions. According to the results presented in Table 5, the increase of all parameters except the condenser pressure has a positive effect on the cycle performance. Therefore, the best mode for this equipment is -20% and vice versa. The results show that the maximum increase in first and second-law efficiencies that can be achieved relative to the nominal conditions is about 20% for the steam cycle. For the combined cycle, these values are about 6% and 8%, respectively.

5 Conclusions

This research presents energy and exergy analyses of a real steam power plant in Iran, aiming to replace an existing boiler with a HRSG fed by a gas turbine unit. The study investigates the effects of various parameters on the first and second-law efficiencies of each unit and the overall system. This research yielded several significant findings, including:

- 1 The analysis of the existing steam cycle reveals that the boiler accounts for 90% of total exergy destruction, followed by the steam turbine at 5.35%. The condenser only accounts for 3% of total exergy destruction. Six heaters and the boiler contribute 25% and 70% to the turbine's input energy, respectively. The boiler and condenser both have the lowest second-law efficiencies at about 45%. Heaters number 4 and 6, the main pump and turbine achieve the highest second-law efficiencies.
- 2 By replacing the existing boiler with a HRSG, the thermal efficiency of the steam cycle is increased from 37.74% to 65.06%, and the exergy efficiency is also increased from 39.3% to 65.27%.
- 3 The study indicates that a 27.5 kPa increase in condenser vacuum pressure results in a 5% decrease in the cycle's overall efficiency.
- 4 The temperature of steam entering the turbine directly impacts the power plant's output. A 3% increase in energy efficiency and a 2% increase in exergy efficiency occur for every 55-degree temperature increase in both steam and combined cycles. Exergy efficiency also increases from the HP turbine to the LP turbine, as the irreversibility of exergy in the LP turbine is lower than in the IP and HP turbines. Therefore, increasing the number of turbine stages will increase the exergy efficiency of the turbine.
- 5 The thermal efficiencies of steam and combined cycles increase by 6% and 4% with an increase in the inlet temperature to the IP turbine by 176°C, primarily due to improved boiler performance.
- 6 The study found that changes in boiler outlet pressure up to 103 bar can increase the first and second law efficiencies by about 5% and 4%, respectively, for both steam and combined cycles. This is a reduction of the exergy destruction rate in the boiler, resulting in a reduction of the total destruction rate of the cycle.
- 7 The study indicates that for $\pm 20\%$ variation of the studied parameters with respect to the nominal conditions, the optimal efficiency is achieved when both T11 and T14 are increased by 20%, resulting in improvements of 16% and 6% in steam and combined cycle efficiencies. The maximum efficiency can be achieved at about 20% when all parameters are in optimal conditions.

References

- Adibhatla, S. and Kaushik, S.C. (2017) 'Energy, exergy and economic (3E) analysis of integrated solar direct steam generation combined cycle power plant', *Sustainable Energy Technologies and Assessments*, April, Vol. 20, pp.88–97.
- Aljundi, I.H. (2009) 'Energy and exergy analysis of a steam power plant in Jordan', *Applied Thermal Engineering*, Vol. 29, Nos. 2–3, pp.324–328.
- Arpit, S., Kumar, P., Prasanta Kumar, D.A.S. and Dash, S.K. (2021) 'Application of exergy analysis in understanding the performance of a coal-fired steam power plant (120 MW) with single reheat and regenerative configuration', *Journal of Thermal Engineering*, Vol. 9, No. 2, pp.497–509.
- Atiz, A., Karakilcik, M. and Erden, M. (2023) 'Daily energetic, exergetic, electricity, and environmental analyses of photovoltaic thermal panel integrated with parabolic trough solar collector in four months', *International Journal of Exergy*, Vol. 41, No. 4, pp.352–375.
- Azubuikwe, U.G., Egbuhuzor, L.C., Njoku, H.O. and Ekechukwu, O.V. (2023) 'Exergy analysis of a steam power plant at full and partial load conditions', *International Journal of Exergy*, Vol. 40, No. 2, pp.182–197.
- Cengel, Y., Boles, M.A. and Kanoğlu, M. (2019) *Thermodynamics: An Engineering Approach*, 9th ed., in SI Units, McGraw-Hill, New York, NY, USA.
- Davoodi, V., Deymi-Dashtebayaz, M. and Rad, E.A. (2023) 'Multi-objective optimisation of a transient solar absorption chiller from energetic, exergetic, and economic viewpoints', *International Journal of Exergy*, Vol. 42, No. 2, pp.159–178.
- Deymi-Dashtebayaz, M., Ebrahimi-Fizik, A. and Valipour-Namanlo, S. (2019) 'Energy and exergy analyses of using natural gas compressor station waste heat for cogeneration power and fresh water', *International Journal of Exergy*, Vol. 30, No. 2, pp.139–156.
- Erzen, S., Ibrahim Acar, H. and Pektezeli, O. (2022) 'Exergy analysis of a coal-fired thermal power plant in Kangal District of Turkey', *International Journal of Exergy*, Vol. 39, No. 3, pp.262–279.
- Kapooria, R.K., Kumar, S. and Kasana, K.S. (2008) 'Technological investigations and efficiency analysis of a steam heat exchange condenser: conceptual design of a hybrid steam condenser', *Journal of Energy in Southern Africa*, Vol. 19, No. 3, pp.35–45.
- Khaleel, O.J., Ibrahim, T.K., Ismail, F.B., Al-Sammarraie, A.T. and Abu Hassan, S.H. (2022) 'Modeling and analysis of optimal performance of a coal-fired power plant based on exergy evaluation', *Energy Reports*, Vol. 8, pp.2179–2199.
- Khaliq, A., Islam, S. and Dincer, I. (2019) 'Energy and exergy analyses of a HCCI engine-based system running on hydrogen enriched wet-ethanol fuel', *International Journal of Exergy*, Vol. 28, No. 1, pp.72–95.
- Klein, S.A. and Alvarado, F. (2018) *EES: Engineering Equation Solver*, F-chart software, Madison, Wisconsin.
- Manesh, M.H.K., Kabiri, S. and Yazdi, M. (2020) 'Exergoenvironmental analysis and evaluation of coupling MSF, MED and RO desalination plants with a combined cycle plant', *International Journal of Exergy*, Vol. 33, No. 1, pp.76–97.
- Mert, S.O., Demir, M.H., Demir, H.G. and Kok, C. (2023) 'Energy, exergy, and exergoeconomic analysis of a general UAV', *International Journal of Exergy*, Vol. 41, No. 4, pp.376–390.
- Mohseni, M. and Bazargan, M. (2014) 'Entropy generation in turbulent mixed convection heat transfer to highly variable property pipe flow of supercritical fluids', *Energy Conversion and Management*, November, Vol. 87, pp.552–558.
- Pinto, G.M. et al. (2022) 'Exergy analysis of a natural gas combined cycle power plant: a case study', *International Journal of Exergy*, Vol. 37, No. 2, pp.159–180.
- Rout, I.S., Gaikwad, A., Verma, V.K. and Tariq, M. (2013) 'Thermal analysis of steam turbine power plants', *IOSR Journal of Mechanical and Civil Engineering (IOSR-JMCE)*, Vol. 7, No. 2, pp.28–36.

- Siddiqui, P. (2021) 'Energy and exergy analyses of a large capacity supercritical utility boiler system', *International Journal of Exergy*, Vol. 34, No. 1, pp.103–124.
- Surywanshi, G.D., Pillai, B.B.K., Patnaikuni, V.S., Vooradi, R. and Anne, S.B. (2020) 'Energy and exergy analyses of chemical looping combustion-based 660 MWe supercritical coal-fired power plant', *International Journal of Exergy*, Vol. 31, No. 1, pp.14–33.
- Vakilabadi, M.A., Bidi, M. and Najafi, A. (2018) 'Energy, exergy analysis and optimization of solar thermal power plant with adding heat and water recovery system', *Energy Conversion and Management*, Vol. 171, pp.1639–1650.
- Naserabad, S.N., Mehrpanahi, A. and Ahmadi, G. (2019) 'Multi-objective optimization of feed-water heater arrangement options in a steam power plant repowering', *Journal of Cleaner Production*, Vol. 220, pp.253–270.